Carbohydrate Polymers 85 (2011) 759–764

Contents lists available at ScienceDirect

Carbohydrate Polymers

journal homepage: www.elsevier.com/locate/carbpol

Influence of drying temperature and duration on fiber properties of unbleached wheat straw pulp

Yang-mei Chen[a,c,*], Jin-quan Wan[a,b,c], Ming-zhi Huang[a,b,d], Yong-wen Ma[a,b,c,*], Yan Wang[a,c], Hui-lin Lv[b], Jing Yang[b]

[a] College of Environmental Science and Engineering, South China University of Technology, Guangzhou 510006, PR China
[b] State Key Lab Pulp and Paper Engineering, South China University of Technology, Guangzhou 510640, PR China
[c] The Key Lab of Pollution Control and Ecosystem Restoration in Industry Clusters, Ministry of Education, China, Guangzhou 510006, PR China
[d] College of Chemistry and Chemical Engineering, South China University of Technology, Guangzhou, 510640, PR China

ARTICLE INFO

Article history:
Received 24 January 2011
Received in revised form 28 February 2011
Accepted 25 March 2011
Available online 2 April 2011

Keywords:
Wheat straw fiber
Drying
Crystallinity of cellulose
Water retention value
Pore structure

ABSTRACT

Plant fibers are mainly composed of cellulose, lignin and hemicelluloses. Fiber swelling ability (water retention value) of unbleached wheat straw pulp and crystal structure of cellulose were studied for different drying temperature and duration. A low-temperature nitrogen adsorption method was employed to analyze the change of pore structure of the wheat straw fiber after drying. A transmission electron microscope (TEM) was used to characterize the change in the ultrastructure of fiber cell walls during drying. An increase of either variable (drying temperature or drying time) is harmful to the quality of the fiber, leads to a decrease in the swelling property of the pulps, the increases of crystallinity of cellulose and the lactones content, and to deformation and collapse of the fiber cell wall.

1. Introduction

Plant fibers is the most abundant renewable and biodegradable carbohydrate polymer in the nature which have the complex composite structures that are mainly composed of cellulose, lignin and hemicelluloses (Liu et al., 2008; Rowell, Pettersen, Han, Rowell, & Tshabalala, 2005). It is known that the polymeric constituents and their organization have a significant influence on the fibers. As resource shortages and environmental problems become more serious, the use of recycled plant fiber is being given attention globally. Recycled fiber has become a very important part of paper materials in China, accounting for more than one third of total paper fibrous materials, and the proportion has been increasing. It is estimated that China recycled about 17 million tones of paper in 2005. A ton of recycled plant fiber (waste paper) saves 3 m^3 of wood, 50% of the process water, 60–70% of the chemicals and more than 50% of the energy needed to make new paper from virgin pulp papers (Gu, 2002). Therefore, increasing the use of recycled plant fiber is an effective means for reducing deforestation and pollution.

Cellulose is a polymer chain formed of cellobiose base units (Clark, 1985). The cellobiose units form a long, flat polymer chain that exposes a number of hydroxyl groups, bonding sites that allow the polymer chain to form a large amount of hydrogen bonds (Smook, 1982). Cellulose pulp drying is a complex and important operation, which influences the structure and properties of paper. Different drying rates and temperatures can affect the fiber water retention value (WRV) (Iyer, Sreenivasan, Chidambareswaran, Patil, & Sundaram, 1991; Nazhad & Paszner, 1994). As early as 1963, Robertston found that high temperature drying could cause WRV decrease (Robertson, 1963); Hillis also reached the same conclusion through high temperature treatment of wood pulp fiber (Hillis, 1984). In addition, Matsuda et al. investigated the effects of thermal and hydrothermal treatments on the reswelling capabilities of pulps and papersheets (Matsuda, Isogai, & Onabe, 1994). The authors found that WRV decreased with increasing temperature and time of treatment, and also found that the decrease of WRV is brought about primarily by formation of hydrogen bonds in non-crystalline regions of cellulose and hemicellulose in the papersheets but without any additional crystallization.

Bhuiyan et al. studied the changes of crystallinity of drying wood cellulose by heat treatment and found that crystallinity increased initially and then decreased with increased processing times (Bhuiyan, Hirai, & Sobue, 2000). Nazhad and Paszner thought that the increase of crystallinity was due to some parts of amorphous regions being converted to crystalline regions after the fiber

* Corresponding authors at: College of Environmental Science and Engineering, South China University of Technology, Guangzhou 510006, PR China.
Tel.: +86 20 87114970; fax: +86 20 39380560.
E-mail addresses: chenyangmei_2001@sina.com (Y.-m. Chen), ppywma@scut.edu.cn (Y.-w. Ma).

0144-8617/$ – see front matter © 2011 Elsevier Ltd. All rights reserved.
doi:10.1016/j.carbpol.2011.03.041

drying process; the authors verified that drying is mainly responsible for the damage of the fiber in the recycling process (Nazhad & Paszner, 1994). Matsuda et al. studied the changes of crystallinity before and after drying by wide-angle X-ray diffraction (XRD) method and found the crystallinity did not significantly change (Matsuda et al., 1994). Researchers have not reached a consensus about the effect of drying on crystallinity of cellulose.

The pore size and pore size distribution in the fiber wall are influenced by mechanical and chemical treatments such as beating, drying and the use of wet strengthening agents. These treatments modify the cell wall structure and affect fiber properties such as swelling ability and flexibility. For example, the fibers shrink in the dryer section of the paper machine and fibrils in the fiber wall move closer to each other (Weatherwax, 1977). This results in almost complete pore closure of dried cellulose fibers. Stone et al. thought that high temperature caused the pore structure of fiber to deform and caused a loss of fiber flexibility (Stone & Scallan, 1968). Häggkvist et al. studied the influence of drying on the pore structure of cellulose fiber wall by ^{1}H and ^{2}H NMR and found that the average pore size of fiber cell wall decreased as the water content of fiber decreased during the drying process (Häggkvist, Li, & Ödberg, 1998). Different methods can be used to characterize the cell wall pores. A commonly used method is the solute exclusion technique (Böttger, Thi, & Krause, 1983). Other techniques, such as inverse size exclusion chromatography (Aggerbrandt & Samuelsson, 1964; Berthold & Salmén, 1997), the NMR relaxation method (Li & Eriksson, 1994; Li & Henriksson, 1993; Maloney, Li, & Weise, 1997) and low-temperature nitrogen adsorption (Hu, Che, Yang, Liu, & Huang, 2003; Liu et al., 2005; Ren, Zhang, Jiang, & Yu, 2007; Yang, Luo, & Xu, 2006) can be also used. In this study, nitrogen adsorption was performed to investigate possible differences in the pore size and pore size distribution of cellulose samples at different drying conditions.

Most of above researchers mainly focused on wood pulps. Very little research was carried out on non-wood pulps, especially wheat straw pulp, one of the main raw materials for pulp and paper in China and accounting for one-third of China's pulp (Chen, Wang, Wan, & Ma, 2010; Gu, 2002). Accordingly, it is important to study the changes of properties of non-wood fibers during drying.

The objective of this work was to determine the effects of different drying conditions (temperature and time) on the swelling ability, crystal structure, pore structure and ultrastructure of wheat straw fiber.

2. Materials and methods

2.1. Materials and sample preparation

Wheat straw was laboratory cooked in an 18-liter digester using a conventional soda-anthraquinone process. Cooking was carried out under conditions (800 g o.d. wheat straw, maximum temperature of 158 °C, 90 min time to the temperature, 30 min time at temperature, 14% NaOH, 0.05% anthraquinone, liquor-to-straw ratio of 4/1). Unbeaten and unbleached wheat straw pulp was used with a moisture content of 82% by weight in the never-dried state. Use of never-dried pulp was considered important, since a high water content protects cellulose crystallites from mechanical damage (Wijnman, 1954). The lignin content, the average fiber length, fines content of the unbleached wheat straw pulp were 10.9%, 0.58 mm and 3.31%, respectively.

Handsheets were made on a British hand sheet machine according to Tappi standards. The basis weight of unbleached wheat straw pulp paperboard was 200 g/m^2. For the drying temperature tests, handsheets were dried at 60 °C, 80 °C, 100 °C, 120 °C for 15 min, respectively; for drying time tests, samples were dried at 100 °C for 5 min, 10 min, 15 min, 20 min and 30 min, respectively. The handsheets were re-wetted by soaking in deionized water for at least 8 h and then disintegrated for 30,000 revolutions in a disintegrator.

2.2. Determination of crystallinity of cellulose by X-ray diffraction

The X-ray diffraction (XRD) scattering pattern of the pulp was analyzed on a Philipps X'Pert MPD diffractometer using a Cu-Kα source ($\lambda = 0.154$ nm) in the 2θ of range 4–40° and a scanning step width of 0.02°/scan. Each analysis was repeated in triplicate. The phone scattering was subtracted from the pulp diffraction diagram. The crystalline reflections and amorphous halo were defined according to previously described recommendations (Rebuzzi & Evtuguin, 2006). The degree of cellulose crystallinity (α) and the average width of crystallite in the 0 0 2 lattice plane were calculated as follows:

$$\text{Crystallinity } \alpha, \% \frac{I_{cr}}{I_{cr} + I_{am}} \times 100 \quad (1)$$

$$L_{002} = \frac{K\lambda}{\beta_\theta \cos\theta} \quad (2)$$

where I_{cr} and I_{am} are the scattering intensities from the crystalline and amorphous regions of cellulose, respectively; β is the width in the middle height of the 0 0 2 reflection, rad; θ is the maximum of the 0 0 2 reflection, rad; λ is the wavelength of X-ray source (0.154 nm); K is the Scherer constant (0.9).

2.3. Determination of water retention value

The water retention value was determined by a centrifugal method with 1.5 g samples (o.d.). The pulp was centrifuged at 3000 × g for 15 min and then weighted before and after drying. The WRV is calculated as follows:

$$\text{WRV} = \frac{m_1 - m_2}{m_2} \times 100\% \quad (3)$$

where m_1 is the weight of wet pulp after centrifugation and m_2 is the weight of dry pulp.

2.4. Low-temperature nitrogen adsorption method

Prior to testing, the samples were freeze-dried in order to remove free water. This procedure aids in preserving the pore structure of the fiber (Chen et al., 2010; Pachulski & Ulrich, 2007). In this study, a pore size distribution detector ASAP2010 M (USA, Micromeritics) was used for structural analyses of the fiber pores. High-purity N_2 was used as absorbate and the adsorption–desorption of high-purity N_2 was determined at 77 K in a liquid nitrogen trap using a static volumetric method. This approach was applied to obtain adsorption–desorption isotherms for the non-recycled and recycled fibers. Subsequently, calculations based on the BET equation (Brunauer–Emmett–Teller), using BJH mode, H-K mode, DFT (density functional theory), T-plot, etc., were used to analyze the specific surface area of the porous materials, the sizes of the macropores, mesopores, and micropores, the total pore volume and average pore size, and surface structural parameters.

2.5. Transmission electron microscope: sample preparation and topographic observation

Wheat straw fiber was fixed over 24 h in a 4% glutaraldehyde fixative solution prepared with 0.1 M sodium phosphate buffer, and washed six times with 0.1 M sodium phosphate buffer. These samples were then fixed overnight in 1% osmium acid stationary liquid prepared with 0.1 M sodium phosphate buffer and washed six times with the same buffer. The mixture was dehydrated in

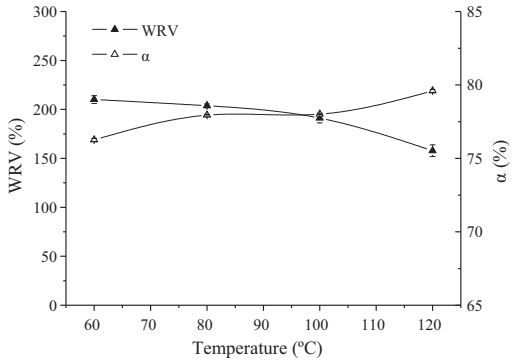

Fig. 1. Effect of drying temperature on WRV and the crystallinity of cellulose.

an ethanol gradient (30, 50, 70, 80, 90, and 100%, three times (20 min at each concentration), then subjected to an epoxy propane (EP) transition (20 min, three times), and then to EP infiltration (EP812 = 3:10.5 h); EP812 = 1:11 h; EP812 = 1:32.5 h). The samples were kept in pure EP overnight (changed once or twice in the process) and then embedded, with polymerization carried out at 60 °C for 72 h. The embedded block was allowed to sit at room temperature for one week. The optimal sites for obtaining semi-thin sections were determined by optical microscopy. The sections were sliced using a Leica-S type ultramicrotome, double-stained with 2% uranium acetate (1 h) and lead citrate (20 min), and observed and imaged using a JEM-1010 transmission election microscope.

2.6. Determination of lactones content in pulps

The lactones content was determined according to a previously published method (Ruffini, 1966; Stakheeva-Kaverzneva & Salova, 1953).

3. Results and discussion

3.1. Effects of drying on crystal structure and WRV of the unbleached wheat straw fiber

As shown in Fig. 1, the crystallinity of cellulose increased and the WRV decreased with an increase in drying temperature, in accordance with the previous results (Bhuiyan et al., 2000; Matsuda et al., 1994). As the drying temperature was increased from 60 °C to 120 °C, the crystallinity of cellulose of unbleached wheat pulp increased by 4.4% and the WRV decreased by 24.9%.

Fig. 2 shows the effect of drying time on WRV and crystallinity. The longer the drying time, the smaller the WRV and the larger the crystallinity. The crystallinity increased by 5.8% and WRV decreased by 52.2% when the drying time was increased from 5 min to 30 min.

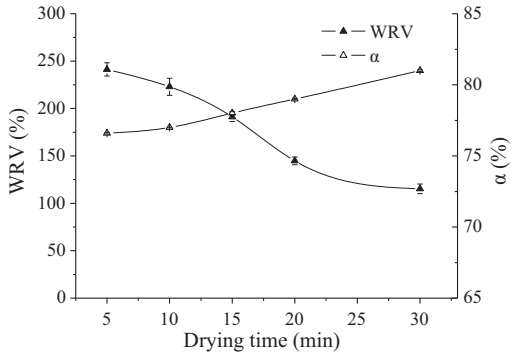

Fig. 2. Effect of drying time on WRV and the crystallinity of cellulose.

Table 1
Effect of drying temperature on L_{002} average width of crystallite.

Drying temperature (°C)	60	80	100	120
L_{002} (nm) ± SD	5.2 ± 0.1	5.6 ± 0.2	5.9 ± 0.1	6.2 ± 0.1

SD = Estimated standard deviation of the mean.

The decrease in the WRV with increasing drying degree might have been due to the formation of irreversible hydrogen bonds in the cellulose fibrils of the pulp fiber during the drying step to form paper, or to irreversible aggregation of cellulose microfibrils, or perhaps both factors (Hult, Larsson, & Iversen, 2001; Matsuda et al., 1994; Wistara & Yong, 1999).

The average width of crystallite in the 0 0 2 lattice plane (L_{002}) was increased with an increase in drying temperature (Table 1), suggesting that the cocrystallization of crystallite had occurred in the fibrils. Some of the amorphous regions and paracrystal regions were converted into regular crystalline regions during drying, which might also have led to an increase in cellulose crystallinity. An increase in crystallinity due to the ordering of paracystalline cellulose on the crystallite surface has been suggested also by other authors (Wistara, Zhang, Young, 1999).

3.2. Effect of drying on the formation of lactones

It is known that a hydroxycarboxylic acid can undergo intramolecular esterification to yield a cyclic ester, called a lactone (Streitwiser & Heathcock, 1989). The formation of lactones in cellulosic materials induced by drying has been reported (Slavik & Kucerova, 1967, 1969). The presence of lactone was qualitatively detected through the pink color in the hydroxylamine-ferric chloride test in hornified pulps (Stakheeva-Kaverzneva & Salova, 1953) but not detected in never-dried pulps (Ruffini, 1966). The quantitative determination of lactones was performed colorimetrically or through the variation of the carboxylic acid content. The formation of lactones is an alternative interpretation of hornification.

As shown in Table 2, the lactones content of pulps increased with the increasing drying temperature. When the drying temperature was increased from 60 °C to 120 °C, the lactones content of unbleached wheat pulp increased from 6.5 mmol/kg to 9.6 mmol/kg. The formation of lactones will result in the loss of fiber swelling ability. This covalent crosslinking is not broken by water molecules and will only disappear under the specific chemical conditions that reverse lactone formation.

The lactones content also increased with increased drying time (Table 2). The lactones content was increased by 24.3% when the drying time was 20 min, compared with the drying time was 5 min.

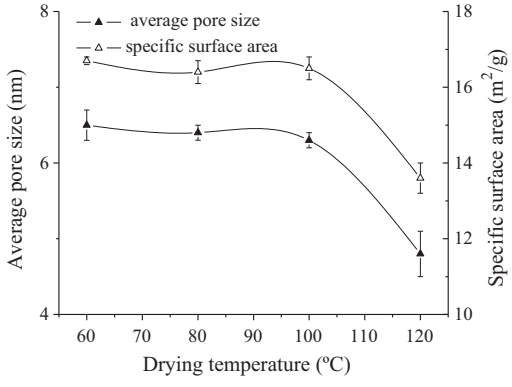

Fig. 3. Average pore size and BET surface area of unbleached wheat straw fiber at different drying temperature.

Table 2
Effect of drying on the lactones content.

Drying temperature (°C)	60	80	100	120	
Lactones content (mmol/kg ± SD)	6.54 ± 0.15	7.23 ± 0.10	8.16 ± 0.12	9.57 ± 0.23	
Drying time (min)	5	10	15	20	30
Lactones content (mmol/kg ± SD)	7.89 ± 0.10	8.05 ± 0.06	8.16 ± 0.12	9.43 ± 0.15	9.81 ± 0.12

SD = Estimated standard deviation of the mean.

3.3. The average pore size and BET specific surface area at different drying conditions

Drying can affect pore structure of fiber to some extent. Fig. 3 and Fig. 4 show that the average pore size and BET specific surface area of unbleached wheat straw pulp in different drying temperature or duration. Average pore size and the BET specific surface area are relatively common parameters used to characterize the pore structure of porous materials (Maloney, 1999). The pore size of the fiber cell wall can influence fiber elastic modulus and the ability of the fiber to adsorb chemical additives (Häggkvist et al., 1998).

The hornification is evident for the unbleached wheat straw pulp after drying. The WRV decreased with the increase in drying temperature or duration of the unbleached wheat straw pulp (see Fig. 1 and Fig. 2). As seen in Fig. 3 and Fig. 4, the average pore size of the fiber decreased with an increase in drying temperature or duration. Especially, the average pore size dramatically decreased when the drying temperature was 120 °C, or the drying time was 20 min. The average pore size was decreased by 26.2% when the drying temperature was increased from 60 °C to 120 °C. Similarly, the average pore size was decreased by 37.3% when the drying time was increased from 0 min to 20 min. It is evident that average pore size is shifted to smaller pore size. These results are in accordance with other researchers' results (Chen et al., 2010; Lindström & Carlsson, 1982; Laivins & Scallan, 1993). They also suggested that the effect of hornification is shown as a decrease in both the average pore size and the WRV after drying.

The sum of the internal surface area of the micropores, mesopores, and macropores of fiber cell walls is the fiber specific surface area. In this study, the specific surface area of the pulp fiber decreased with the drying temperature or duration increase resulting in the decrease in accessibility of the fiber. This overall decrease in the specific surface area of the fiber was due to irreversible closure of the pores of the fiber cell wall.

3.4. Effect of drying temperature on the pore size distribution of wheat straw fiber

Gregg and Sing divided the pores of porous solids into three groups: micropores (radius: <2.0 nm), mesopores (radius: 2–50 nm), macropores (radius: >50 nm) (Gregg & Sing, 1982).

Fig. 5 shows that pore sizes were mainly distributed between 2 nm and 300 nm after drying. When the drying temperature was up to 120 °C, some micropores small than 2.0 nm were seen. The pore size decreased with an increase in the drying temperature and pore volume modes were in the range of 2–5 nm. The temperature had a significant effect on the proportion of mesopores, especially between 2 and 10 nm. As the drying temperature was increased from 60 °C to 80 °C, from 80 °C to 100 °C and from 100 °C to 120 °C, the average pore volume corresponding to mesopores decreased by 7.4×10^{-5} cm^3/g, 3.22×10^{-5} cm^3/g and 5.42×10^{-5} cm^3/g, respectively. The results showed that mesopores were found predominantly in fibers. The pore volume corresponding to mesopores decreased with an increase in the drying temperature. The effect of drying temperature on fiber pore was mainly located in the mesopores.

Fig. 5 shows the pore structure of fiber changed greatly at different drying temperature, which led to the decrease in WRV. This can be ascribed to fiber pore closure which results from collapse of the cell wall, and the increase of the degree of irreversible bonding and increase in the degree of fiber decay. Accordingly, a lower drying temperature can be applied with no negative effect on the swelling property and structure of fiber.

3.5. Effect of drying time at 100 °C on the pore size and pore size distribution of wheat straw fiber

As shown in Fig. 6, pore sizes were mainly distributed between 1.5 nm and 300 nm. Pore volume modes were in the range of 1.5–4 nm for the various drying times. The fiber pore volume decreased with an increase in drying time, which had a notable effect on the proportions of fiber mesopores, especially between 2 and 30 nm. In addition, average pore volume corresponding to mesopores and micropores between 1.5 and 8 nm decreased by 4.2×10^{-5} cm^3/g when the drying time was increased from 10 min to 15 min. The average pore volume corresponding to mesopores and micropores at 10 min was higher than the average pore volume at 15 min. From Fig. 6 it can also seen that pore size distributions

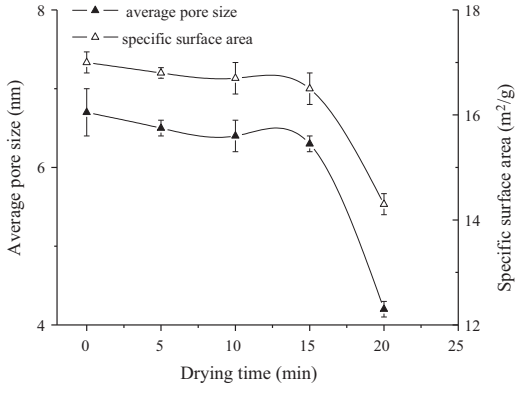

Fig. 4. Average pore size and BET surface area of unbleached wheat straw fiber at different drying times.

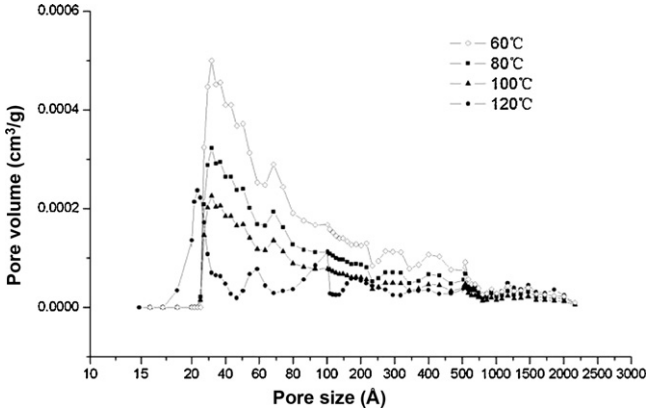

Fig. 5. Effect of drying temperature on pore size and pore size distribution of fibers (drying time 15 min).

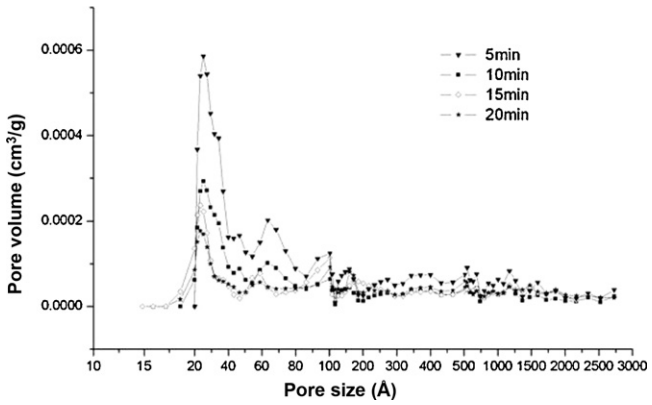

Fig. 6. Effect of the drying time on pore size and pore size distribution of fibers (drying temperature 100 °C).

were almost coincident for drying times of 15 min and 20 min. This indicates that the pore structure changed insignificantly after about 15 min.

The degree of irreversible pore closure was enhanced with increasing drying time. The reason was that higher temperatures can promote a change from elastic to plastic deformation in the pore structure of the cell walls, which influences the adsorption of free water by fiber and reduces the capacity for swelling in water. Hence there is a decrease in fiber quality.

3.6. TEM analysis of ultrastructure of fiber

The TEM image shows the cell walls of plant fiber are successively primary wall (P), secondary wall (S) and lumen (L), from outer to inner. The secondary wall is divided into outer secondary (S1), middle secondary (S2) and inner secondary (S3). As shown in Fig. 7, the stratification of wheat straw fiber was obvious, the primary wall was very thin and the secondary wall was thick. However, the outer, middle and inner stratification in the secondary wall was hardly evident.

Jang et al. investigated dried fiber by confocal laser scanning microscopy (CLSM) (Ho & Reza, 1994; Jang, 1997). The authors found that deformation and collapse of the cell lumen of fiber were obvious. So, drying affects the morphological structure of fiber. In this work, TEM was used to study the change in the morphological structure of fiber after drying and rewetting. Fig. 8 shows a photo of a transverse section of wheat straw fiber after drying and rewetting was obtained by TEM. It can be seen that there were obvious deformation and collapse of cell lumen in unbleached straw fiber after rewetting, which were not reversible unless treated. This is due to the evaporation of water immersed in the voids of cell walls in papermaking treatments, so that surface tension pulls the cell walls together and pores collapse closed larger voids. Adhesion of pore walls to each other resulted in lamination of cell wall lamellae. The collapse of the cell wall was not reversible. When fibers contacted water again, they cannot completely swell to their original volumes.

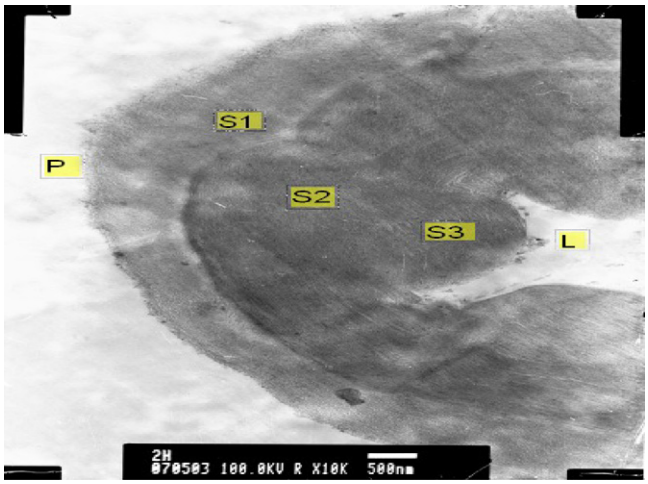

Fig. 7. Configuration of the cell wall on the virgin wheat straw fiber.

Fig. 8. Transverse section of wheat straw fiber after drying and rewetting.

4. Conclusions

Drying conditions influence wheat straw fiber properties. The crystallinity of cellulose and the lactones content increased, and the water retention value of fiber decreased, with an increase in the drying temperature or duration. The average width of crystallite in 0 0 2 lattice plane (L_{002}) increased with higher drying temperatures, which shows that co-crystallization of crystallites maybe occurs in fibrils during drying. This resulted in the increase of the crystallinity of cellulose.

The drying temperature affected mesopores of fiber had a significant effect, but had little effect on pore size distribution. The degree of irreversible closure of pore structure of fiber increased with increase of drying temperature or duration.

Unbleached wheat straw fiber, analyzed by transmission electron microscope, shows a deformed and collapsed surface, and a less porous surface after drying and rewetting. Moreover, the deformation and collapse were irreversible.

Acknowledgements

This work was supported by the National Technology Research and Development of China (863 Programme) (No. 2007AA03Z433), Science and Technology Key Project of Guangdong Province, China (No. 2008A0302008), Science and Technology Plan Project of Guangdong Province, China (No. 2008B030302035) and The Key Lab of Pollution Control and Ecosystem Restoration in Industry Clusters, Ministry of Education, China.

References

Aggerbrandt, L. G., & Samuelsson, O. (1964). Penetration of water-soluble polymers into cellulose fibers. *Journal of Applied Polymer Science, 8*(6), 2801–2812.

Berthold, J., & Salmén, L. (1997). Inverse size exclusion chromatography (ISEC) for determining the relative pore size distribution of wood pulps. *Holzforschung, 51*(4), 361–368.

Bhuiyan, M. T. R., Hirai, N., & Sobue, N. (2000). Changes of crystallinity in wood cellulose by heat treatment under dried and moist conditions. *Journal of Wood Science*, *46*, 431–436.

Böttger, J., Thi, L., & Krause, T. (1983). Untersuchungen zur porenstruktur von zellstoffasern. *Das Papier*, *37*(10A), 14–21.

Chen, Y. M., Wang, Y., Wan, J. Q., & Ma, Y. W. (2010). Crystal and pore structure of wheat straw cellulose fiber during recycling. *Cellulose*, *17*, 329–338.

Clark, J. D. A. (1985). *Pulp technology and treatment for paper* (2nd ed.). San Francisco, California: Miller Freeman Publications.

Gregg, S. J., & Sing, K. S. W. (1982). *Adsorption surface area and porosity* (2nd ed.). London: Academic Press.

Gu, M. D. (2002). Suggestions on the expansion of waste paper reclamation. *China Pulp and Paper Industry*, *24*(5), 17–19.

Häggkvist, M., Li, T. Q., & Ödberg, L. (1998). Effects of drying and pressing on the pore structure in the cellulose fiber wall studied by ^{1}H and ^{2}H NMR relaxation. *Cellulose*, *5*(1), 33–49.

Hillis, W. E. (1984). High temperature and chemical effects on wood stability. Part1: Generalconsiderations. *Wood Science and Technology*, *18*(4), 281–289.

Ho, F. J., & Reza, A. M. (1994). Fiber characterization using confocal microscopy-collapse behavior of mechanical pulp fibers. *Tappi Journal*, *79*(4), 203–210.

Hu, B. L., Che, Y., Yang, Q., Liu, D. M., & Huang, W. H. (2003). Analysis on cryogenic nitrogen isothermal adsorption characteristic of coal reservoirs in the Ordos Basin. *Coal Geology and Exploration*, *31*(2), 20–23.

Hult, E. L., Larsson, P. T., & Iversen, T. (2001). Cellulose fibril aggregation – an inherent property of kraft pulps. *Polymer*, *42*, 3309–3314.

Iyer, P. B., Sreenivasan, S., Chidambareswaran, P. K., Patil, N. B., & Sundaram, V. (1991). Induced crystallization of cellulose in never-dried cotton fibers. *Journal of Applied Polymer Science*, *42*(6), 1751–1757.

Jang, H. F. (1997). Using confocal microscopy to characterize the collapse behavior of fibers. *Tappi Journal*, *81*(5), 167–173.

Laivins, G. V., & Scallan, A. M. (1993). The mechanism of hornification of wood pulps. In C. F. Baker (Ed.), *Products of papermaking* (pp. 1235–1260). Leatherhead, UK: Pira International.

Li, T. Q., & Eriksson, U. (1994). Kaolin-based coating layer studied by ^{2}H and ^{1}H NMR relaxation method. *Langmuir*, (10), 4624–4629.

Li, T. Q., & Henriksson, U. (1993). Determination of pore sizes in wood cellulose fibers by ^{2}H and ^{1}H NMR. *Nordic Pulp & Paper Research Journal*, *8*(3), 326–330.

Lindström, T., & Carlsson, G. (1982). The effect of carboxyl groups and their ionic form during drying on the hornification of cellulose fibers. *Svensk Papperstidn*, *85*(15), 146–151.

Liu, D. T., Li, J., Yang, R. D., Mo, L. H., Huang, L. H., Chen, Q. F., et al. (2008). Preparation and characteristics of moulded biodegradable cellulose fibers/MPU-20 composites ($CFMC_S$) by steam injection technology. *Carbohydrate Polymers*, *74*, 290–300.

Liu, H., Wu, S. H., Jiang, X. M., Wang, G. Z., Cao, Q. X., Qiu, P. H., et al. (2005). The configuration analysis of the adsorption isotherm on nitrogen in low temperature with the lignite char produced under fast pyrolysis. *Journal of China Coal Society*, *30*(4), 507–510.

Maloney, T. C. (1999). The formation of pores in the cell wall. *Journal of Pulp and Paper Science*, *25*(12), 430–436.

Maloney, T. C., Li, T. Q., & Weise, U. (1997). Paulapuro H. Intra- and inter-fiber pore closure in wet pressing. *Appita Journal*, *50*(4), 301–306.

Matsuda, Y., Isogai, A., & Onabe, F. (1994). Effects of thermal and hydrothermal treatments on the reswelling capabilities of pulps and papersheets. *Journal of Pulp and Paper Science*, *20*(11), 323–327.

Nazhad, M. M., & Paszner, L. (1994). Fundamentals of strength loss in recycled paper. *Tappi Journal*, *7*(9), 171–179.

Pachulski, N., & Ulrich, J. (2007). New fields of application for sol-gel process cold and vaccum-free 'compacting' of pharmaceutical materials to tablets. *Chemical Engineering Research and Design*, *85*(A7), 1013–1019.

Rebuzzi, F., & Evtuguin, D. V. (2006). Effect of glucuronoxylan on the hornification of Eucalyptus globulus bleached pulps. *Macromolecular Symposia*, *232*, 121–128.

Ren, G. P., Zhang, C. Q., Jiang, X. M., & Yu, L. J. (2007). Analysis of surface area and pore structure of Datong Coal. *Combusition Science and Technology*, *13*(3), 265–268.

Robertson, A. A. (1963). The physical properties of wet webs. *Svensk Papperstidn*, *66*(12), 477–497.

Rowell, R. M., Pettersen, R., Han, J. S., Rowell, J. S., & Tshabalala, M. A. (2005). Cell wall chemistry. In R. M. Rowell (Ed.), *Wood chemistry and wood composites* (pp. 35–74). New York: Taylor & Francis.

Ruffini, G. (1966). Improvement in bonding of wood pulps by the presence of acidic groups. *Svensk Papperstidn*, *69*, 72–76.

Slavik, I., & Kucerova, M. (1967). Formation of lactone bonds in cellulose during acidification and drying. *Faserforsch Textiltechnology*, *18*, 396–397.

Slavik, I., & Kucerova, M. (1969). Time profile of lactone and ester formation in cellulose upon acidification and drying. *Faserforsch Textiltechnology*, *20*, 346–347.

Smook, G. A. (1982). *Handbook for pulp and paper technologists*. Montreal, Quebec, Canada: Canadian Pulp and Paper Association.

Stakheeva-Kaverzneva, E. D., & Salova, A. (1953). Specific method of determination of carbonyl groups in oxycellulose. *Zhur Anal Khim*, *8*, 365–369.

Stone, J. E., & Scallan, A. M. (1968). A structural model for the cell wall of water swollen wood pulp fibers based on their accessibility to macromolecules. *Cellulose Chemistry and Technology*, *2*(3), 343–349.

Streitwiser, A., & Heathcock, C. H. (1989). *Introduction to organic chemistry* (3rd ed.). New York: Macmillan., p. 859.

Weatherwax, R. C. (1977). Collapse of cell-wall pores during drying of cellulose. *Journal of Colloid Interface Science*, *62*(3), 432–446.

Wijnman, C. F. (1954). Influence of heavy beating of cotton fibers on molecular length and crystallinity. *Tappi*, *37*, 96–99.

Wistara, N., & Yong, R. A. (1999). Properties and treatments of pulps from recycled paper. Part I: Physical and chemical properties of pulps. *Cellulose*, *6*, 291–324.

Wistara, N., Zhang, X. J., & Young, R. A. (1999). Properties and treatments from recycled paper. Part II. Surface properties and crystallinity of fibers and fines. *Cellulose*, *6*(4), 325–348.

Yang, T. Z., Luo, S. Z., & Xu, Y. S. (2006). Characterization of pore structure based on N_2 adsorption applied to porous materials. *Carbon*, (1), 17–22.